Journal of Petroleum Exploration and Production Technology (2023) 13:995–1007
https://doi.org/10.1007/s13202-022-01599-7

ORIGINAL PAPER - EXPLORATION GEOLOGY

Petroleum source rock potential evaluation: a case study of block 11a, Pletmos sub-basin, offshore South Africa

F. A. Agbor[1] · S. Mhlambi[1] · N. A. Teumahji[2] · W. A. Sonibare[3] · J. M. van Bever Donker[1]

Received: 21 June 2022 / Accepted: 20 December 2022 / Published online: 19 January 2023

Abstract

Among the several existing geochemical methods in hydrocarbon exploration, the technique linking total organic carbon content (TOC) and Rock–Eval pyrolysis is most widely used, largely as a result of its capacity to rapidly provide vital information regarding the identification of source rocks and their defining characteristic, as well as thermal maturity levels and generative potentials. In this study, data from prospective source units within the southern depocenter of the Pletmos Sub-basin were analyzed using this geochemical method. Cutting samples from six wells in Block 11a were subjected to organic geochemical analysis to understand the occurring hydrocarbon scenario. Based on the results of the investigation, five notable source rock intervals of Kimmeridgian to Turonian ages were identified. The source rocks are shales with both indigenous and non-indigenous organic matter. Their TOC values show a fair to excellent petroleum generating potential, with the Aptian and Kimmeridgian intervals having the highest and lowest, respectively. The Hydrogen Index (HI), along with S_2/S_3 ratio values, typifies a predominance of mixed type II/III (oil/gas-prone) with some type III (gas-prone) and II (oil-prone) kerogens. The trends of the maturity parameters T_{max} and Ro (vitrinite reflectance) indicate maturities ranging from immature to a late stage of maturity (dry gas window). Two observed breaks in the Ro profile reveal a possible link of maturity to high heat flow that is allied to sedimentation and tectonic uplift during the Late Cretaceous. Generally, based on TOC, S_1, and HI, the petroleum potential trend increases with increasing depth, with a striking display of mixed hydrocarbon generating potential. Interpreted hydrocarbon typing is thus recommended to support the well-testing analysis.

Keywords Geochemistry · Source rock evaluation · Thermal maturity · Hydrocarbon generation · Block 11a · Pletmos Basin

Introduction

Establishing a predictive model for generation and charge within a petroleum system is one of the first phases in any exploration work program in a sedimentary basin (Hantschel and Kauerauf 2009; Al-Hajeri et al. 2009). This begins with a comprehensive examination of the characteristics of potential hydrocarbon source rocks, such as the amount, type, and degree of organic matter conversion to petroleum (Hantschel and Kauerauf 2009; Peters et al. 1994). Such data are critical for the identification of possible contributors to existing hydrocarbons and evaluating prospects within the basin. This paper attempts to establish existing prospective source rocks and examine their total organic carbon (TOC) weighted percentage contents, organic matter types, and levels of thermal maturity (Ro) within Block 11a of the Pletmos Sub-basin ('the Basin'). The proliferous sub-basin spanning approximately 18,000 km^2 is centrally located within the wider Outeniqua Basin (Fig. 1) and amid the most promising areas for exploration, up to 200 m isobath line (Roux and Davids 2009; Fig. 1).

Hydrocarbon exploration within the basin began in the late 1960s, and the operator, SOEKOR (now part of the state oil company of South Africa), has conducted extensive work within the southern depocenter (McMillan et al. 1997; Roux 1997). The earliest wells in the basin primarily targeted structural and stratigraphic traps associated

✉ F. A. Agbor
2947208@myuwc.ac.za

[1] Department of Earth Sciences, University of the Western Cape, Cape Town, South Africa

[2] Schlumberger GmbH, Aachen, Germany

[3] Schlumberger Ltd., Southern Africa, Cape Town, South Africa

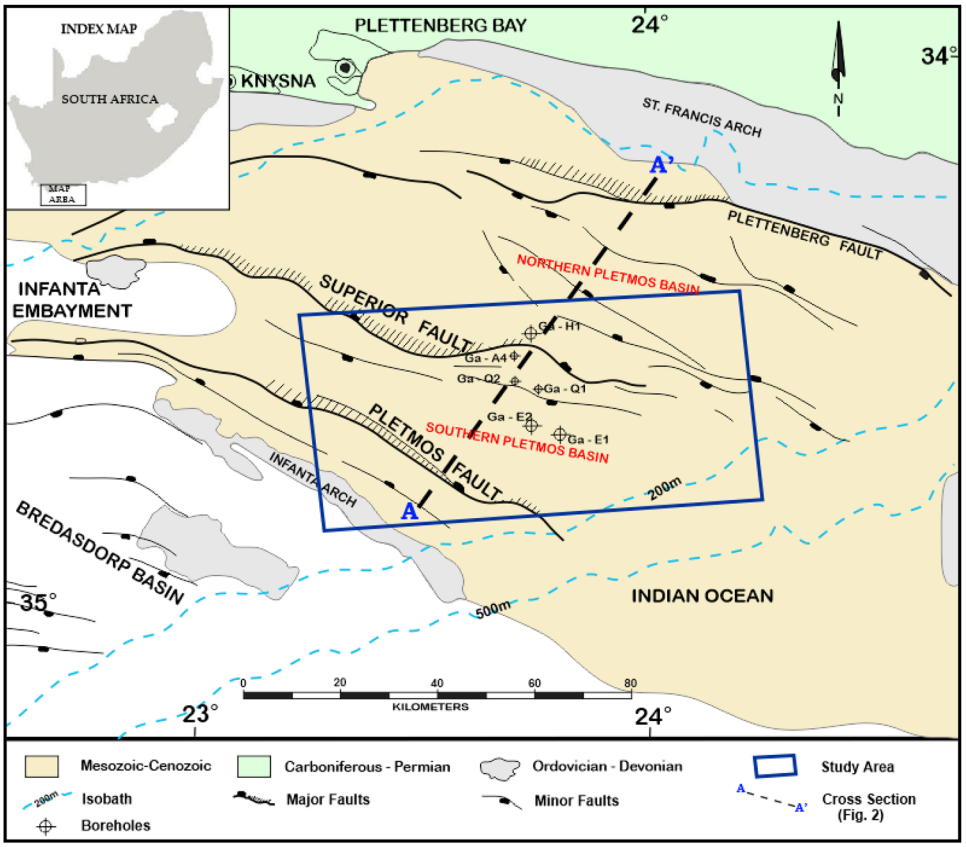

Fig. 1 The location map highlighting the approximately 1025 km^2 within the southern depocenter of the Pletmos Basin. Modified after Bate and Malan (1992) and Viljoen et al. 2010

with shallow marine sandstone reservoirs of syn-rift Upper Jurassic age. Some of these wells exhibited a few oil, gas and condensate shows, thus establishing a working petroleum system (Brown et al. 1996; McMillan et al. 1997; Roux 1997). Source rocks in the region consist of fine-grained clay-rich siliciclastic rocks (i.e., mudstones and shales) proven to have generated and effectively expelled hydrocarbons (Davies 1997a, b; Roux and Davids 2009).

Albeit the proven potential, the basin remains relatively under-explored (Broad et al. 2006). Further prospecting that targeted post-rift Cretaceous reservoirs within prograding wedges incised valley fills, slope fans, and low stand basin floor fans encountered only minor hydrocarbon shows. Likewise, charging seems to have occurred within specific areas and from various sources of different maturity levels within the sedimentary fill (McMillan et al. 1997; Roux 1997). Consequently, a thorough analysis of the meagrely available data from the offshore wells is necessary. While significant studies have been carried out in the area of study, no work utilizing well-known integrated geochemical analytic tools of TOC and Rock–Eval pyrolysis to assess and fully Interpret available data, identify the possible source rocks, ascertain their hydrocarbon productive potential, and estimate the maturity levels within the location of study is available in the public domain.

Geologic setting

The Pletmos (together with the Bredasdorp, Gamtoos, Algoa, and Southern Outeniqua sub-basins) makes up the Outeniqua intra-cratonic rift basin (Bate and Malan 1992; McMillan et al. 1997; Roux and Davids 2009; Viljoen et al. 2010; Sonibare et al. 2015a, b). These sub-basins are considered to have formed during the Middle to Late Jurassic as a result of extensional forces related to the break-up of Gondwana (Fig. 1; McMillan et al. 1997; Roux and Davids 2009; Sonibare et al. 2015a, b). Their spatial distribution decreases systematically from west to east, and they are separated by fault-bounded basement arches comprised primarily of Ordovician Cape Supergroup, Cape granite, and Pre-Cambrian metamorphic rocks (van der Merwe and Fouché 1992; McMillan et al. 1997; Roux 1997; Thomson 1998; Broad et al. 2006; Roux and Davids 2009). They possess boundary fault networks (Fig. 2) whose strike directions gradually change from primarily east–west to north–south.

The Pletmos Basin is structurally more complex than the other sub-basins of the Outeniqua Basin and spans an area of approximately 18,000 km^2 (Brown et al. 1996; McMillan et al. 1997; Broad et al. 2006). Its major-bounding Superior Fault separates the basin into two

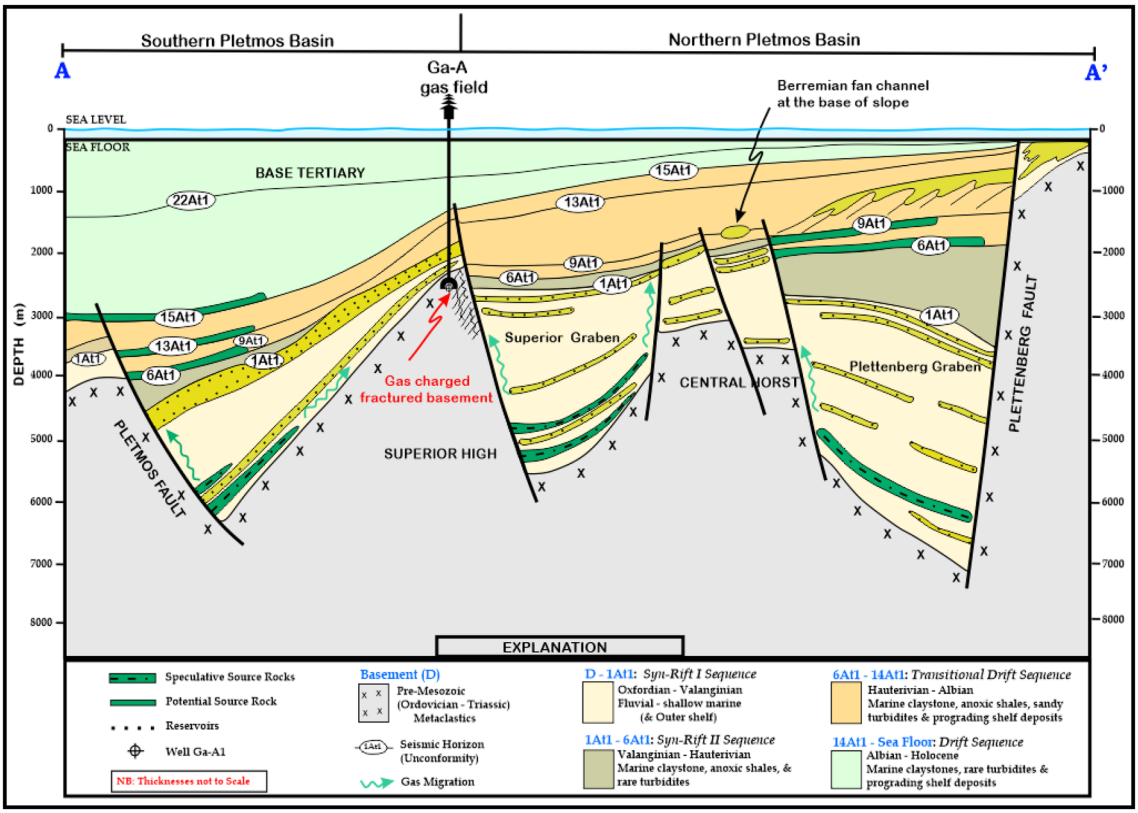

Fig. 2 Schematic section across the Pletmos Basin, illustrating structural styles and stratigraphic subdivision adapted from Roux and Davids (2009). The major faults shown arose from the rifting associated with the break-up of Gondwana and maintained significant structural constraints throughout the Cretaceous period (Brown et al. 1996; McMillan et al. 1997)

major depocenters and, along with the other two major bounding faults (the Pletmos and Plettenberg Faults, to the southwest and northeast, respectively), defined the limits of rift sedimentation in the Basin (Fig. 2). Evidently, distinct sub-basins existed to the north and south of the fault during the rift phase (Brown et al. 1996; McMillan et al. 1997; Viljoen et al. 2010).

The absence of a complete drilled sequence, coupled with the rapid variations in the earliest sediment facies of depocenters, has hampered a comprehensive understanding of the pre-rift history of the basin (McMillan et al. 1997). On the basis of drilled wells that stretched into the basin's shallow basement, however, three stages of sedimentation namely: the rift, transitional-early drift, and late drift phases (Fig. 2), have been identified and are linked to the syn-rift and post-rift tectonic mega-sequences (Figs. 2, 3). In addition, it is anticipated (Brown et al. 1996; McMillan et al. 1997) that the basin-wide unconformities—Horizon D, 1At1 (drift-onset unconformity) and the mid-Aptian 13At1—represent the onset of these episodes and are crucial for the stratigraphic and petroleum system development in the basin (Brown et al. 1996; McMillan et al. 1997; Davies 1997a,b; Broad et al. 2006; Sonibare et al. 2015b).

The basin-fill is subdivided according to tectonic phases into generally isolated fault-bounded syn-rift sequences overlain by post-rift sediments of a varied thickness (Fig. 2). As predicted (e.g., Burden 1992; Davies 1997b; Roux 2007; Sonibare et al. 2015b), the current structural configuration of this region (Fig. 2) is presumed to be the result of mixed tectonic and sedimentary processes, including continental break-up, uplift, subsidence, mantle dynamics, denudation, sediment dispersal, and accretion.

The chronostratigraphic sequence (Fig. 3) outlines the tectonic phases and associated depositional and erosional events during the duration of the basin's development.

Sampling and methodology

Data

Six offshore wells, namely Ga-A4, Ga-E1, Ga-E2, Ga-H1, Ga-Q1, and Ga-Q2, located in Block 11a in water depths ranging from 1080 to 3221 m (Figs. 1, 2), were selected for this study. Laboratory total organic carbon (TOC) and Rock–Eval pyrolysis data on source rock samples from these

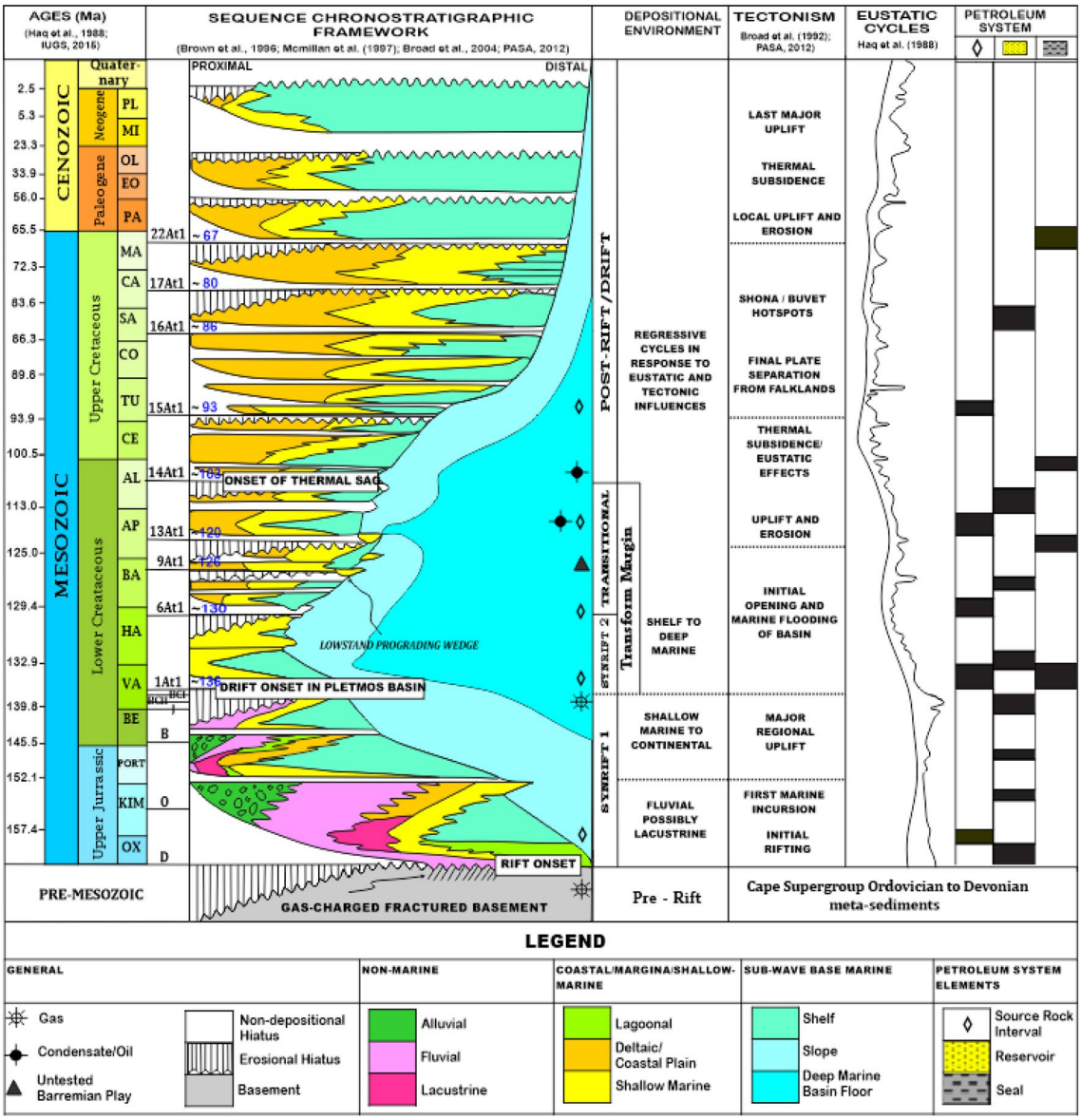

Fig. 3 Chronostratigraphic chart of the Pletmos Basin showing the major depositional and tectonic events in the basin and the prognosed petroleum system elements modified after Brown et al. (1996). The current basin-fill structure is derived from previous research by Brown et al. (1996), McMillan et al. (1997), Broad et al. (2006), Davies (1997a), and Roux (2007). The geologic time scales of Haq et al. (1988) and the International Union of Geological Sciences (IUGS) of 2015 were utilized

wells were obtained from the current operator of Block 11a. A total of ninety (90) samples were chosen for this study; these, together with the Rock–Eval pyrolysis results, are provided in Table 1.

Methods

Using TOC and Rock–Eval pyrolysis data, the samples (Table 1) were systematically studied to assess the quantity, quality, and thermal maturity of the organic matter within these formations. The procedures and analytical Rock–Eval pyrolysis parameters were as published by Peters (1986), Lafargue et al. (1998), Snowdon et al. (1998), and Behar et al. (2001). The Rock–Eval pyrolysis data were utilized since it is the most readily available and provides the tools to identify organic matter type and evaluates the petroleum (oil and gas) potential, generation, and thermal maturity as discoursed by numerous authors (e.g., Tissot and Welte 1978; Espitalie 1985; Peters 1986; Waples et al. 1995; Hunt 1996; Shalaby and Abu Shady 2006).

In general, only samples with TOC values greater than 0.5%, the widely accepted criterion for designating possible

Table 1 Measure Rock–Eval pyrolysis and supplementary derived parameters

Well	#	Depth	S_1	S_2	S_3	S_2/S_3	PI	S_1+S_2	OI	T_{max}	TOC	HI	Ro
Ga-H1	1	1840	0.08	0.63	1.47	0.4	0.11	0.71	161.54	436	0.91	69.23	0.84
	2	1860	0.12	1.07	1.47	0.7	0.10	1.19	124.58	431	1.18	90.68	nr
	3	1880	0.13	1.07	1.58	0.7	0.11	1.2	132.77	435	1.19	89.92	nr
	4	2180	0.09	0.64	1.12	0.57	0.12	0.73	177.78	432	0.63	101.59	nr
	5	2210	0.10	1.21	0.53	2.28	0.08	1.31	80.30	431	0.66	183.33	nr
	6	2220	0.11	0.50	1.25	0.40	0.18	0.61	204.92	432	0.61	81.97	nr
	7	3221	0.44	1.65	1.22	1.35	0.21	2.09	154.43	427	0.79	208.86	1.1
Ga-A4	8	1589	0.43	4.09	0.15	27.27	2.40	4.52	8	428	1.88	218	0.95
	9	1609	0.69	7.23	0.43	16.81	3.19	7.92	17	420	2.48	292	0.87
Ga-Q2	10	1830	0.04	0.64	1.41	0.5	0.06	0.68	87.04	426	1.62	39.51	nr
	11	1830	0.03	0.93	0.98	0.9	0.03	0.96	52.13	436	1.88	49.47	0.7
	12	1840	0.07	1.34	1.1	1.2	0.05	1.41	56.70	426	1.94	69.07	nr
	13	1850	0.06	1.23	1.19	1.0	0.05	1.29	63.64	429	1.87	65.78	nr
	14	1860	0.1	1.64	0.96	1.7	0.06	1.74	48.98	433	1.96	83.67	nr
	15	1870	0.09	1.29	1.55	0.8	0.07	1.38	82.45	433	1.88	68.62	0.7
	16	1880	0.09	1.38	1.55	0.9	0.06	1.47	82.01	433	1.89	73.02	nr
	17	1890	0.09	1.59	1.6	1.0	0.05	1.68	83.77	434	1.91	83.25	0.8
	18	1900	0.09	1.42	1.33	1.1	0.06	1.51	68.21	434	1.95	72.82	nr
	19	1900	0.03	1.2	0.98	1.2	0.02	1.23	60.49	431	1.62	74.07	nr
	20	1910	0.10	1.42	1.32	1.08	0.07	1.52	70.21	429	1.88	75.53	nr
	21	1920	0.08	0.73	1.26	0.58	0.10	0.81	71.59	429	1.76	41.48	nr
	22	1930	0.10	1.35	1.49	0.91	0.07	1.45	83.24	426	1.79	75.42	nr
	23	1940	0.10	1.00	1.18	0.85	0.09	1.10	65.19	431	1.81	55.25	0.8
	24	1940	0.04	0.83	0.24	3.46	0.05	0.87	16.90	431	1.42	58.45	0.87
	25	1950	0.17	1.08	1.75	0.62	0.14	1.25	97.22	427	1.80	60.00	nr
	26	1960	0.09	1.12	1.49	0.75	0.07	1.21	82.32	429	1.81	61.88	nr
	27	1970	0.10	1.11	1.12	0.99	0.08	1.21	61.20	429	1.83	60.66	0.7
	28	1980	0.11	1.04	1.25	0.83	0.10	1.15	71.84	429	1.74	59.77	0.7
	29	1990	0.09	1.03	1.07	0.96	0.08	1.12	61.14	431	1.75	58.86	nr
	30	2000	0.26	2.95	5.80	0.51	0.08	3.21	287.13	431	2.02	146.04	nr
	31	2000	0.12	0.97	1.24	0.78	0.11	1.09	69.66	429	1.78	54.49	nr
	32	2005	0.19	1.36	0.29	4.69	0.12	1.55	14.29	424	2.03	67.00	nr
	33	2033	0.43	10.5	0.80	13.08	0.04	10.89	30.53	429	2.62	399.24	nr
	34	2040	0.21	3.11	1.37	2.27	0.06	3.32	74.05	431	1.85	168.11	nr
	35	2050	0.38	6.20	1.26	4.92	0.06	6.58	62.69	428	2.01	308.46	nr
	36	2060	0.22	4.30	1.60	2.69	0.05	4.52	95.24	431	1.68	255.95	0.73
Ga-Q1	37	1530	0.02	0.55	1.33	0.4	0.04	0.57	127.88	428	1.04	52.88	0.5
	38	1540	0.02	0.43	1.44	0.3	0.04	0.45	158.24	427	0.91	47.25	0.7
	39	1550	0.03	0.97	1.25	0.8	0.03	1	113.64	424	1.10	88.18	nr
	40	1560	0.03	1.14	1.32	0.9	0.03	1.17	99.25	428	1.33	85.71	0.73
	41	1700	0.04	2.54	5.61	0.5	0.02	2.58	316.95	425	1.77	143.50	nr
	42	1710	0.02	0.35	1.2	0.3	0.05	0.37	85.11	424	1.41	24.82	nr
	43	1740	0.03	0.5	1.19	0.4	0.06	0.53	85.00	424	1.40	35.71	0.73
	44	1770	0.03	0.62	1.32	0.5	0.05	0.65	69.84	424	1.89	32.80	nr
	45	1800	0.05	0.5	1.39	0.4	0.09	0.55	85.28	428	1.63	30.67	0.74
	46	1830	0.07	0.53	1.34	0.4	0.12	0.6	69.79	425	1.92	27.60	0.7
	47	1860	0.03	0.42	1.31	0.3	0.07	0.45	79.39	424	1.65	25.45	nr

Table 1 (continued)

Well	#	Depth	S_1	S_2	S_3	S_2/S_3	PI	S_1+S_2	OI	T_{max}	TOC	HI	Ro
	48	1890	0.03	0.4	1.27	0.3	0.07	0.43	75.15	424	1.69	23.67	0.87
	49	1900	0.04	2.0	4.51	0.4	0.02	2.04	241.18	422	1.87	106.95	0.87
	50	1980	0.14	2.38	0.89	2.67	0.06	2.52	64.03	433	1.39	171.22	0.7
	51	1988	0.21	5.81	0.47	12.36	0.03	6.02	22.38	434	2.10	276.67	0.7
	52	1990	0.13	2.00	0.95	2.11	0.06	2.13	65.97	436	1.44	138.89	nr
	53	1999	0.23	3.10	0.22	14.09	0.07	3.33	12.43	426	1.77	175.14	nr
	54	2000	0.14	2.68	0.84	3.19	0.05	2.82	53.85	433	1.56	171.79	nr
	55	2010	0.13	2.52	0.86	2.93	0.05	2.65	65.15	433	1.32	190.91	0.71
	56	2020	0.11	1.50	0.76	1.97	0.07	1.61	64.96	426	1.17	128.21	nr
	57	3249	0.51	1.82	5.90	0.31	1.79	2.33	135	421	1.30	179	1.0
Ga-E2	58	2008.5	0.09	6.15	0.55	11.2	0.01	6.24	24.89	431	2.21	278.28	nr
	59	2653	0.5	3.96	2.41	1.6	0.11	4.46	130.27	431	1.85	214.05	0.75
	60	2657	1.26	16.5	0.66	25.1	0.07	17.8	17.93	436	3.68	449.46	nr
	61	2662	0.57	7.56	0.78	9.7	0.07	8.13	31.58	431	2.47	306.07	nr
	62	2671	0.43	4.84	1.53	3.2	0.08	5.27	73.21	436	2.09	231.58	0.75
	63	2680	0.52	4.02	2.18	1.8	0.11	4.54	110.10	436	1.98	203.03	nr
	64	2692	0.4	4.26	0.97	4.4	0.09	4.66	44.70	436	2.17	196.31	nr
	65	2701	0.61	2.62	1.23	2.1	0.19	3.23	48.62	441	2.53	103.56	0.75
	66	2709	0.45	3.9	0.47	8.3	0.10	4.35	20.35	436	2.31	168.83	0.75
	67	2710	0.61	2.89	1.31	2.2	0.17	3.5	62.38	438	2.1	137.62	nr
	68	2842	0.50	1.82	1.26	1.44	0.22	2.32	63.32	439	1.99	91.46	nr
	69	2851	0.79	3.90	0.91	4.29	0.17	4.69	46.67	441	1.95	200.00	nr
	70	2851	0.52	1.59	0.88	1.81	0.25	2.11	46.07	455	1.91	83.25	nr
	71	2860	0.59	2.22	0.69	3.22	0.21	2.81	32.70	440	2.11	105.21	nr
	72	2872	0.88	3.46	0.60	5.77	0.20	4.34	25.10	436	2.39	144.77	nr
	73	2884	0.62	2.10	0.44	4.77	0.23	2.72	23.28	439	1.89	111.11	nr
	74	2890	0.61	2.29	0.56	4.09	0.21	2.9	27.18	441	2.06	111.17	nr
	75	2900	0.36	1.87	1.00	1.87	0.16	2.23	68.03	444	1.47	127.21	0.7
	76	2902	0.50	1.96	0.71	2.76	0.20	2.46	33.18	442	2.14	91.59	nr
	77	2911	0.69	1.98	0.52	3.81	0.26	2.67	27.08	440	1.92	103.13	nr
	78	2920	0.80	1.90	0.57	3.33	0.30	2.7	28.36	440	2.01	94.53	0.7
	79	2925	0.54	2.52	0.88	2.86	0.18	3.06	53.99	444	1.63	154.60	nr
	80	2932	0.70	2.43	0.94	2.59	0.22	3.13	46.53	455	2.02	120.30	nr
Ga-E1	81	2003.3	0.04	1.11	0.7	1.6	0.03	1.15	58.82	434	1.19	93.28	nr
	82	2462	0.21	0.27	0.88	0.31	0.49	0.48	90	428	0.98	28	0.44
	83	2696	1.15	13.4	0.47	28.5	0.08	14.56	10.47	439	4.49	298.66	0.75
	84	2717	0.68	6.05	0.65	9.31	0.10	6.73	22.18	432	2.93	206.48	nr
	85	2724	1.31	4.21	0.67	6.28	0.24	5.52	24.19	429	2.77	151.99	0.7
	86	2726	0.12	0.91	0.79	1.15	0.12	1.03	54.86	431	1.44	63.19	nr
	87	2756	0.27	1.66	0.46	3.61	0.14	1.93	25.27	437	1.82	91.21	nr
	88	2768	0.33	1.91	0.46	4.15	0.15	2.24	24.47	439	1.88	101.60	nr
	89	2777	0.38	1.82	0.48	3.79	0.17	2.2	26.37	437	1.82	100.00	0.7
	90	2789	0.36	1.92	0.59	3.25	0.16	2.28	30.41	437	1.94	98.97	nr

Depth in mTVD, unless mentioned otherwise: S_1, S_2, S_3 in mg HC/g rock; T_{max} in °C; TOC in wt%; Ro in %; PI production index; OI oxygen index in mg HC/g organic carbon; HI hydrogen index in mg HC/g organic carbon; nr not recorded. # Sample number

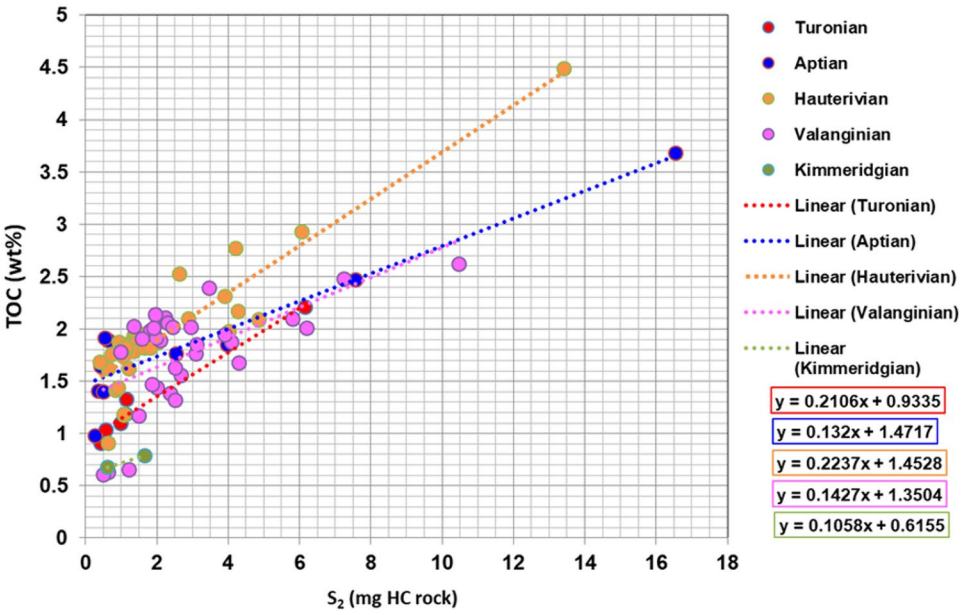

Fig. 4 A plot of S_2 versus TOC for the studied source rocks in Block 11a

source rocks, were deemed eligible for the analysis (Tissot and Welte 1978; Peters and Cassa 1994). Those that have been studied were identified using the conventional criteria for classifying possible source rocks based on S_2 values (e.g., Peters and Cassa 1994; Ibrahimbas and Riediger 2004).

The plot of S_2 values against TOC (Fig. 4; Dahl et al. 2004) was used to determine the inert fraction of the TOC, which was then removed according to the formulae presented in Table 2. However, because TOC diminishes with age, the removal method was done cautiously.

The type of kerogen present was then determined by plotting of hydrogen index (HI) versus oxygen index (OI) on a modified van Krevelen diagram, and thermal maturity was assessed based on pyrolysis T_{max} and vitrinite reflectance measurements (Hunt 1996). Plotting T_{max} against HI highlighted the distinct maturation pathways of the several types of organic matter.

Results and discussion

Prospective source rocks

The identified prospective source rock intervals in the study wells that were included in the analysis are depicted in Fig. 5. Five probable source rock intervals spanning in age from the Lower Jurassic to the Upper Cretaceous were identified and characterized, as illustrated. The average parameter values and interpreted depositional conditions for the various source rock intervals are reported in Table 3.

Table 2 .

Source rocks	Regression line equations	R^2	TOC inert
Turonian	$y = 0.2106x + 0.9335$	0.9638	0.9335
Aptian	$y = 0.132x + 1.4717$	0.8772	1.4717
Hauterivian	$y = 0.2237x + 1.4528$	0.8161	1.4528
Valanginian	$y = 0.1427x + 1.3504$	0.3633	1.3504
Kimmeridgian	$y = 0.1058x + 0.6155$	1	0.6155

Organic matter quantity (Richness)

As high TOC readings do not necessarily indicate superior source rock quality, the threshold of 0.5 wt% TOC for effective shale source rocks was chosen (Tissot and Welte 1984; Peters and Cassa 1994; Hunt 1996; Peters et al. 2005). TOC contents reveal varying degrees of richness, which can be attributed to combined impacts of the environment and burial depth, corroborating well data findings from Petroleum Agency South Africa (PASA 2012).

The results (Fig. 6a, b) indicate the existence of both indigenous and non-indigenous particles (e.g., Ramachandran et al. 2013; Fig. 6b). According to Peters and Cassa (1994) and Law (1999), TOC values for the Kimmeridgian, Valanginian, Hauterivian, and Aptian source rocks are classified as marginal to adequate, with fair values for the Turonian. The Aptian source rock has the highest values, followed by those of the Valanginian, Hauterivian, and Kimmeridgian formations, with the Turonian formation having the lowest values. The ranges of total organic carbon (TOC) for all five source rocks (Fig. 6; Table 1) show that they

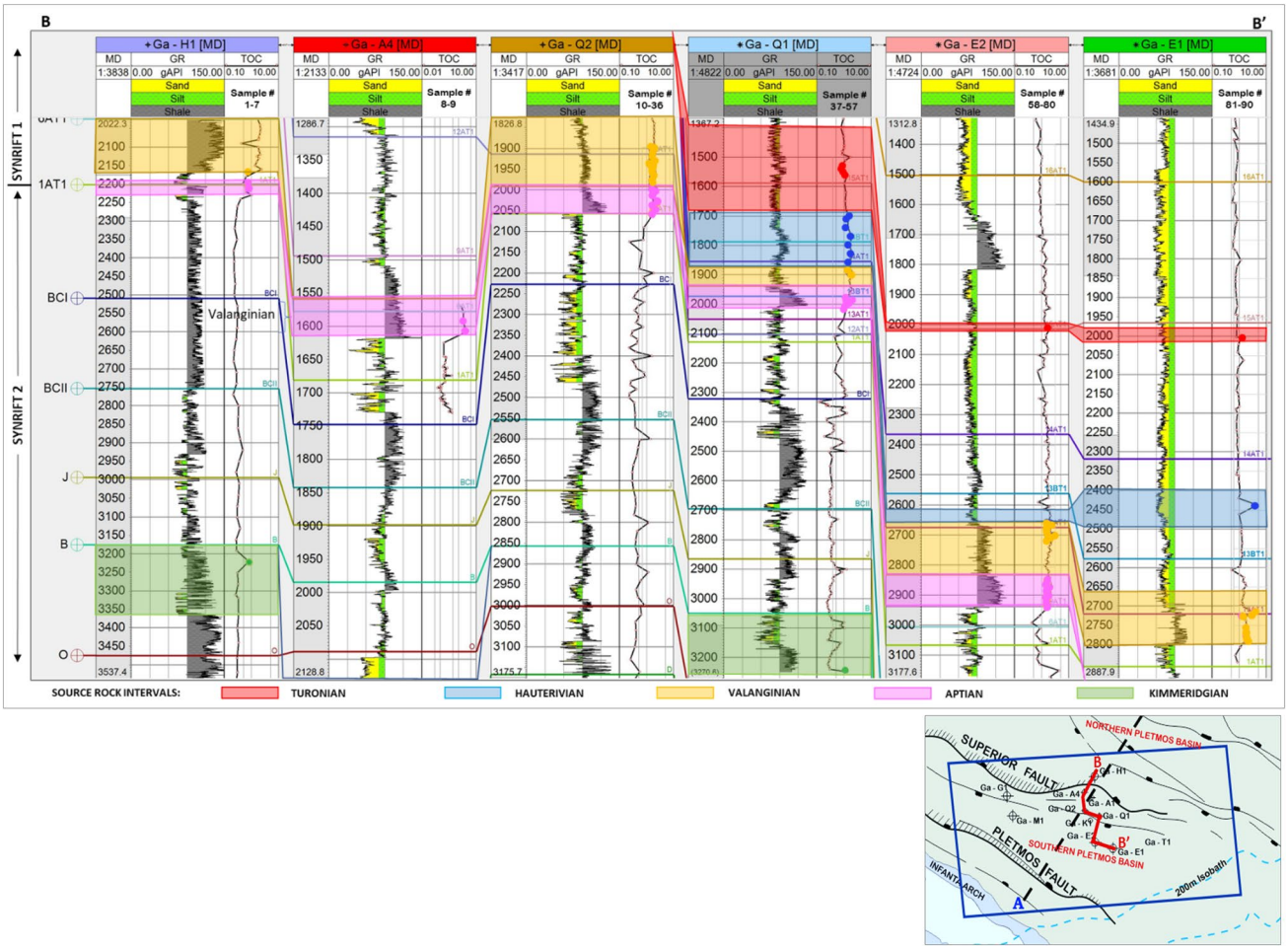

Fig. 5 NW–SE well correlation panel displaying the possible source rock intervals for selected wells within the study area. A reference is shown on the left

Table 3 Organic matter quality and nature of expelled product at peak for the different source rock intervals adapted from Agbor (2017)

Source rock	Depositional environment	Quality of organic matter				Main product expelled at peak maturity
		Kerogen type	HI (mg HC/g TOC)	OI (mg CO2/g TOC)	S_2/S_3 ratio	
Turonian	Inner shelf	III, II/III	47.25–278.28	24.89–158.24	0.3–11.2	Gas, minor oil
Aptian	Slope–deep Marine	III, II	25.45–449.46	17.93–316.95	0.3–25.1	Gas, oil + minor gas
Hauterivian	Deep marine (abyssal plain)	III, II	23.67–298.66	10.47–241.18	0.3–28.5	Gas, oil + minor gas
Valanginian	Deep marine (abyssal plain)	III, II	54.49–399.24	8.00–287.13	0.4–27.27	Gas, oil + minor gas
Kimmeridgian	Lacustrine	III, II/III	179–208.86	135–154.43	0.31–1.35	Gas, minor oil

match the generally accepted criteria for fair to excellent potential to generate petroleum.

After accounting for the wt% of inert carbon (Table 2), the TOC values for the source formations range from 0.68–0.79 wt%, averaging 0.74 wt% for the Kimmeridgian; 0.61–2.48 wt %, averaging 1.55 wt% for the Valanginian; 0.91–4.49 wt%, averaging 2.70 wt% for the Hauterivian; 0.98–3.68 wt%, averaging 2.33 wt% for the Aptian; and 0.91–2.21 wt%, averaging 1.62 wt% for the Turonian (Fig. 6).

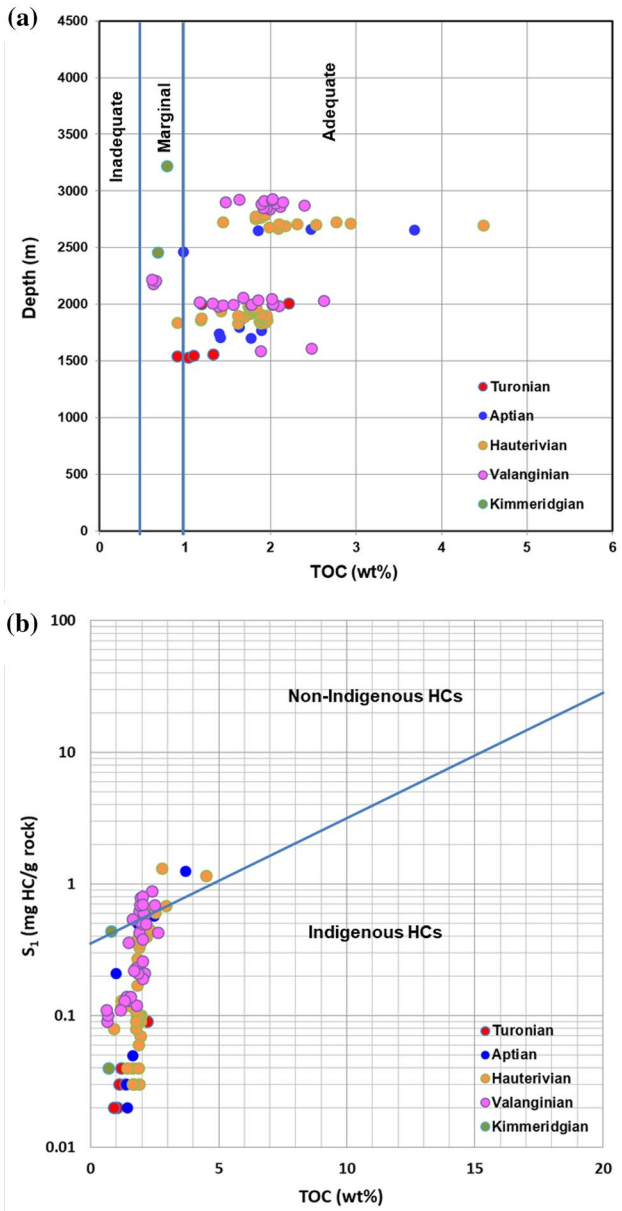

Fig. 6 Analyzed sample distribution plots demonstrating **a** the total organic carbon (wt%) content versus depth and **b** indicating indigenous and non-indigenous hydrocarbons

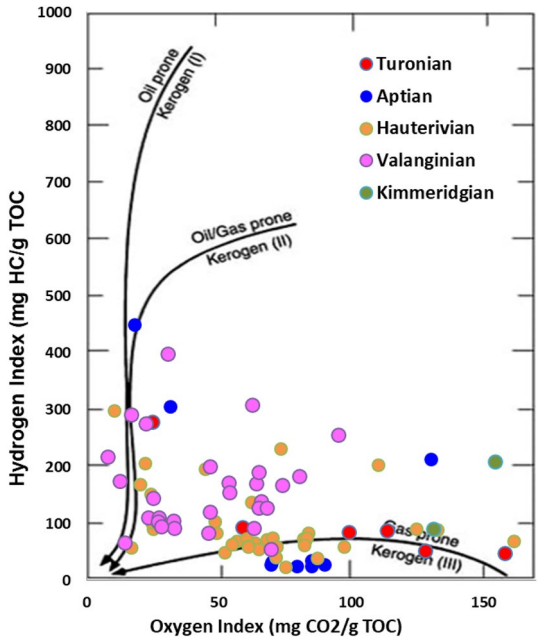

Fig. 7 Cross-plot of sample distribution illustrating kerogen types (quality) with the character of expelled products at peak maturity adapted from Agbor (2017)

Organic matter quality (type)

The HI composition of the kerogens in the source rock governs the quantity and type of hydrocarbons generated during thermal maturation. Consequently, the assessment of the organic matter type in a source unit is a crucial evaluation factor for petroleum source rocks (Hunt 1996; Peters 1986). The most common way to achieve this purpose is to plot HI values versus OI values (Fig. 7).

Accordingly, the general trend in Fig. 7 demonstrates a mixture and predominance of type II and type III kerogen dispersion. This signifies terrestrial and marine organic matter origin and presence, which is substantiated by HI values ranging from 23.67 to 449.46 (mg HC/g TOC). The analyzed Kimmeridgian and Turonian samples are predominantly type II and type III, respectively. The Aptian formation is a mix of types II and III, whereas the Valanginian and Hauterivian formations are type II/III, respectively.

The observed variation can may be attributed to the mixing of organic matter from various sources, as well as reworking and deposition in a highly oxidizing environment. Despite this, the Aptian source rock exhibits exceptionally high S_2/S_3 values, indicating that oil is likely to be the expelled product during peak maturity.

Maturity evaluation and vitrinite reflectivity analysis

The plotting of T_{max} versus HI vales has been widely used to evaluate the thermal maturity of source rocks (e.g., Espitalié 1985; Tissot and Welte 1984; Jarvie 1991; Peters and Cassa 1994; Law 1999; McCarthy et al. 2011). To efficiently evaluate the thermal maturity of the source rocks in this study, a combination of HI, T_{max}, and vitrinite reflectance was employed. Figure 8 indicates that the Aptian and Turonian formations are less mature than the Kimmeridgian, Valanginian, and Hauterivian source rock units, in accordance with their stratigraphic burial depths and locations.

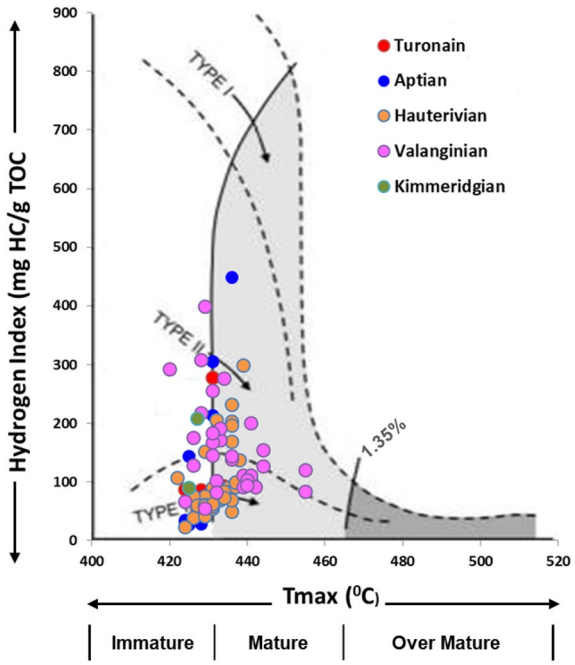

Fig. 8 Cross-plot of Rock–Eval T_{max} versus hydrogen index (HI) showing the range in thermal maturity stages along with kerogen types of the source rock adapted from Agbor (2017)

To validate the maturity results, T_{max} values between 420 and 455 °C (Fig. 9a) were matched with vitrinite reflectance (%VRo) values between 0.5 and 1.1% (Table 4). It is worth noting that %VRo values presented are consistent with peak-late-mature interpretation, particularly for Kimmeridgian samples, although T_{max} values are fairly low. The discrepancy is attributed to the limited number of samples within the Kimmeridgian source interval, which may have resulted in the lack of conformance of T_{max} to the expected thermal evolution trends. Another possible reason for this discrepancy may be due to organic facies changes or source rock chemistry, which have the ability to create data shifts that are not indicative of the trends in maturation. The area is highly fractured and the source rock occurs at separate isolated areas within the two depocenters. As such, the data are not for a uniform source section, hence its uniform character.

For the Mesozoic interval under investigation, 32 vitrinite reflectance samples were available. The %VRo increases significantly with burial depth, and it is seen that the %VRo readings for the Valanginian, at roughly the same depth across the examined wells, increase marginally from 0.70 to 0.90%. This can be attributed to increasing sedimentary unit thicknesses deeper toward the south. Two erosional episodes (Fig. 9b) have been identified as having significant effects on the maturity profile. Importantly, given that the present study area is severely faulted and fractured, this suggests that regions with extensive fracture networks may have experienced a greater basal heat flow.

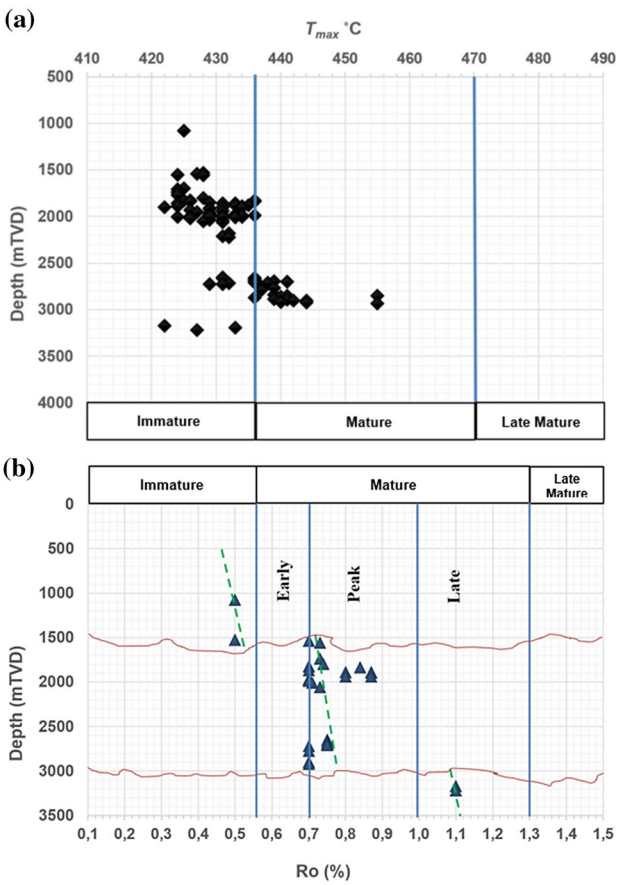

Fig. 9 T_{max} (**a**) and Ro (**b**) depth profile plots indicate two significant erosional breaks in maturity profile, possibly during the uplifts before deposition of overlying formations

Table 4 Characteristic stage of thermal maturity and range values for T_{max} and Vitrinite reflectance for the different source rock intervals adapted from Agbor (2017)

Source rock	Stage of thermal maturity	Maturation	
		Ro (%)	T_{max} (°C)
Turonian	Immature–early mature	0.5–0.73	424–434
Aptian	Immature–peak mature	0.5–0.84	424–436
Hauterivian	Immature–peak mature	0.5–0.70	422–441
Valanginian	Peak mature–late mature	0.7–1.0	420–455
Kimmeridgian	Peak mature–late mature	1.0–1.10	421–427

Hydrocarbon generation potential

The petroleum generative (GP) abilities of source rocks are largely dependent on the original TOC and HI capacities of their kerogens (Peters et al. 2005). Accordingly, the simplest means of determining GP is by plotting genetic potential ($S_1 + S_2$) against TOC values.

In general, ranges of total organic carbon (TOC) for all five source rocks (Fig. 10a; Table 1) indicate that they match the generally accepted criteria for fair to excellent potential for petroleum generation. The sample distribution trends (Figs. 8, 9b) designate a mixture of oil and gas-prone kerogens and signpost an increasing generation potential with depth for the various source rock units.

The relationship between $(S_1 + S_2)$ and TOC data values of the analyzed source rocks indicates a fair to abundant petroleum potential yield and mostly gas-prone kerogen (Fig. 10). Figure 10a indicates a fair to rich mixture of oil and gas, whereas Fig. 10b indicates fair to excellent generation potential for the source samples.

Conclusions

Based on the results from the systematic analysis of the source rock samples, the following conclusion can be drawn:

- The prospective source rocks in the study area have high TOC contents and HI indices, indicating good petroleum generation potentials upon maturation.
- The plot of S_1 against TOC illustrates indigenous and non-indigenous hydrocarbons in the area.
- Although the petroleum potential trend of the source rocks increases with increases with depth, some samples have a mixed hydrocarbon generating potential.
- The data sample parameters suggest the presence of immature to late-mature gas-prone source rocks, with the Turonian source interval remaining predominantly immature. Despite this, due to the small number of samples, the technique employed in this study that links TOC and Rock–Eval pyrolysis data needs to be corroborated by other superior analyses (and modeling studies that captures the geometries and lateral variations of the interval and units) to support the type of hydrocarbons that exist.
- The Kimmeridgian, Valanginian, Hauterivian, and Aptian units are all considered probable source rocks for the reported accumulations in the basin.
- Based on the organic geochemical analysis performed on these source rock samples, the Aptian interval is identified as the most effective petroleum source rock.
- A maturity break identified in the Vitrinite reflectance profile shows that there are roughly two large erosional events with considerable effects. The area is known to be tectonically active; hence, the erosional events are believed to have happened during the periods uplift. In addition, it has been shown that the high temperature and heat flow changes associated with these events have had a major impact on maturity levels. However, alternate interpretations of the break-in Vitrinite reflectance profile might exist. Therefore, data from research such as fluid inclusion and burial history modeling are necessary for the conclusions to be definitive.

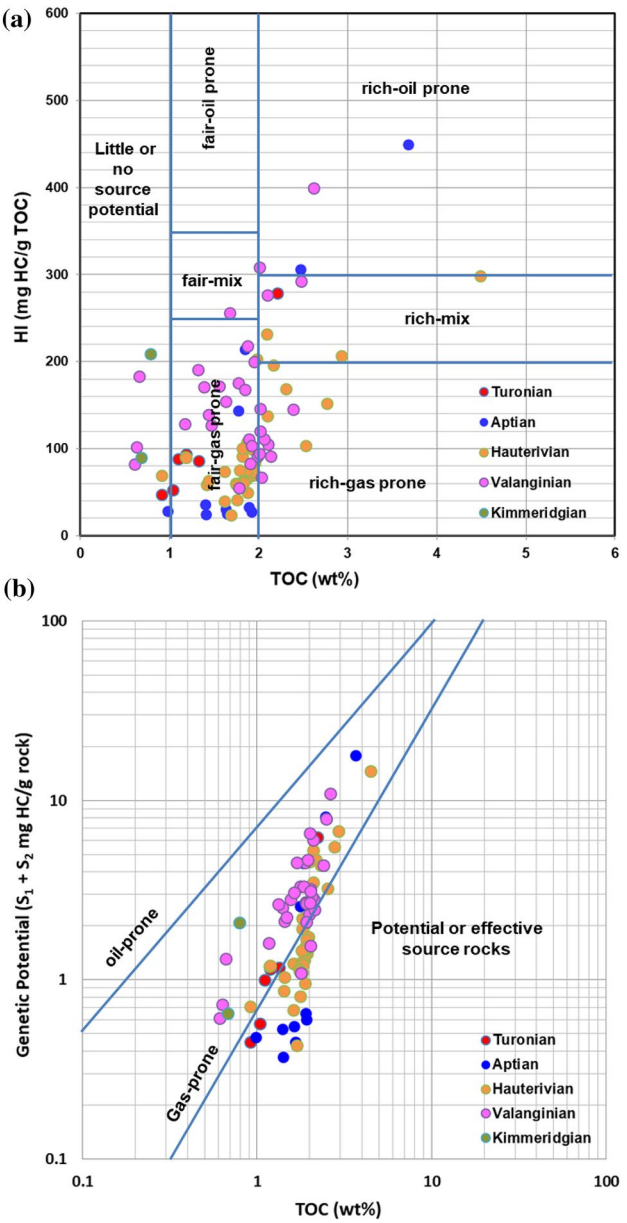

Fig. 10 Plots of analyzed sample distribution demonstrating the petroleum generation potential of the various stratigraphic units within the study area. **a** Displays the representative log that graphically reveals the geochemical information of the wells, which helps to identify the potentially effective source rock intervals within the study area

Acknowledgements We would like to express our deep gratitude to PASA and PetroSA (Soekor Ltd.) for providing the data used, support, and permission to get this paper published. We are also very grateful to the DAAD-NRF and DSI-NRF CIMERA for funding the study in parts through research grants N° 123251 and UID (91487). Thanks are also due to colleagues of the Earth Science department at UWC who shared insights through several brainstorming sessions and those who helped to complete this study.

Funding This study was funded in part by the DSI-NRF through the DAAD-NRF and NRFCIMERA research entities with grants IDs: N° 123251 and UID (91487), respectively.

Declarations

Conflict of interest The authors indicate that there is no conflict of interest with any of the authors or others. Likewise, this manuscript has not been published and is not under consideration for publication elsewhere.

References

Agbor FA (2017) Source Rock analysis, thermal maturation and hydrocarbon generation modelling within the Southern Pletmos Basin, Offshore of South Africa. Dissertation, University of the Western Cape

Al-Hajeri MM, Al Saeed M, Derks J, Fuchs T, Hantschel T, Kauerauf A, Neumaier M, Schenk O, Swientek O, Tessen N, Welte D (2009) Basin and petroleum system modeling. Oilfield Rev 21(2):14–29

Bate KJ, Malan JA (1992) Tectonostratigraphic evolution of the Algoa, Gamtoos and Pletmos basins, offshore South Africa. In: Conference on inversion tectonics of the Cape Fold Belt, pp 61–73

Behar F, Beaumont V, Penteado HD (2001) Rock-Eval 6 technology: performances and developments. Oil Gas Sci Technol 56(2):111–134

Broad DS, Jungslager EHA, Mclachlan IR, Roux J (2006) Geology of the offshore Mesozoic basins. In: Johnson MR et al (eds) The Geology of South Africa. Geological Society of South Africa, Pretoria, pp 553–571

Brown LF Jr, Benson JM, Brink GJ, Doherty S, Jollands A, Jungslager EHA, Keenan JHG, Muntingh A, Van Wyk NJS (1996) Sequence stratigraphy in offshore South African divergent basins. An atlas on exploration for cretaceous lowstand traps by Soekor (Pty) Ltd. Am Assoc Petrol Geol Stud Geol 41:184

Burden PLA (1992) Soekor, partners explore possibilities in Bredasdorp Basin off South Africa. Oil Gas J 90:109–112

Dahl B, Bojesen-Koefoed J, Holm A, Justwan H, Rasmussen E (2004) A new approach to interpreting Rock-Eval S_2 and TOC data for kerogen quality assessment. Org Geochem 35:1461–1477

Davies CPN (1997b) Unusual biomarker maturation ratio changes through the oil window, a consequence of varied thermal history. Org Geochem 27(7/8):537–560

Davies, CPN (1997a) Hydrocarbon evolution of the Bredasdorp Basin, offshore South Africa: from source to reservoir. Dissertation, University of Stellenbosch, pp 286

Hantschel T, Kauerauf AI (2009) Fundamentals of basin and petroleum systems modeling. Springer Science &Business Media

Espitalie J (1985) Use of Tmax as a maturation index for different types of organic matter: comparison with vitrinite reflectance. Collect Colloques Et Séminaires-Institut Français Du Pétrole, Edi Tech, Paris 44:475–496

Haq BU, Hardenbol J, Vail PR (1988) Mesozoic and Cenozoic chronostratigraphy and eustatic cycles of sealevel change. In: Wilgus CK et al (eds) Sea level change: an integrated approach, vol 42. SEPM Special Publications, Tulsa, pp 71–108

Hunt JM (1996) Petroleum geochemistry and geology, 2nd edn. WH Freeman and Company, New York, p 743

Ibrahimbas A, Riediger C (2004) Hydrocarbon source rock potential as determined by Rock-Eval 6/TOC pyrolysis, Northeast British Columbia and Northwest Alberta. British Columbia Ministr Energy Mines Pet Resourc Summ Act 2004:7–17

Jarvie DM (1991) Factors affecting Rock-Eval derived kinetic parameters. Chem Geol 93(1–2):79–99

Lafargue E, Marquis F, Pillot D (1998) Rock-eval 6 applications in hydrocarbon exploration, production, and soil contamination studies. Revue De L'institut Francais Du Petrole 53(4):421–437. https://doi.org/10.2516/ogst:1998036

Law CA (1999) Evaluating Source Rocks. AAPG Special Volumes. Volume Treatise of Petroleum Geology/Handbook of Petroleum Geology: Exploring for Oil and Gas Traps

McCarthy K, Rojas K, Niemann M, Palmowski D, Peters K, Stankiewicz A (2011) Basic petroleum geochemistry for source rock evaluation. Oilfield Rev 23(2):32–43

McMillan IK, Brink GJ, Broad DS, Maier JJ (1997) Late Mesozoic sedimentary basins off the south coast of South Africa. In: Selley RC (ed) African basins. Sedimentary Basins of the World, vol 3. Elsevier Science B.V., Amsterdam, pp 319–376

PASA (2012) Petroleum exploration in South Africa: information and opportunities. PASA, Cape Town, p 30

Peters KE (1986) Guidelines for evaluating petroleum source rocks using programmed pyrolysis. Am Assoc Pet Geol Bull 70(3):318–329

Peters KE, Cassa MR (1994) Applied source rock geochemistry: chapter 5: Part II. Essential elements. Am Assoc Pet Geol Mem 60:93–12

Peters KE, Cassa MR, Magoon LB, Dow WG (1994) The petroleum system—From source to trap. Am Assoc Pet Geol Mem 60:93–120

Peters KE, Clifford CE, Moldowan JM (2005) The biomarker guide, 2nd edn. Prentice-Hall, New Jersey

Ramachandran K, Babu V, Behera BK, Harinarayana T (2013) Source rock analysis, thermal maturation, and hydrocarbon generation using rock-eval pyrolysis in parts of Krishna-Godavari basin, India: a case study. J Pet Explo Prod Tech 3(1):11–20

Roux J (1997) Soekor (Pty) Ltd, Exploration and Production: Potential Outlined in Southern Outeniqua Basin, off S Africa. Oil Gas J 95(29):87–91

Roux J, Davids A, (2009) PS Barremian basin floor fan complex: an untested gas play within the Northern Pletmos Basin

Roux J (2007) Republic of South Africa 2007 license round- Area C: Proximal Bredasdorp Basin. Petroleum Agency South Africa, p 26

Shalaby MR, Abu Shady AN (2006) Thermal maturity and timing of oil generation of source rocks in Shams oil field, North Western Desert, Egypt. Middle East Res Cent Ain Shams Univ Earth Sci Ser 20:97–116

Snowdon LR, Fowler MG, Riediger CL (1998) Interpretation of organic geochemical data. CSPG Short Course Notes, Calgary, Alberta

Sonibare WA, Sippel J, Scheck-Wenderoth M, Mikeš D (2015a) Crust-scale 3D model of the Western Bredasdorp Basin (Southern South Africa): data-based insights from combined isostatic and 3D gravity modelling. Bas Res 2:125–151. https://doi.org/10.1111/bre.12064

Sonibare, WA, di Primio, R, Anka, Z, Scheck-Wenderoth, M, Mikeš, D (2015b) Petroleum systems evolution within a transform-related passive margin setting: crustal-scale 3D basin modelling of the Western Bredasdorp Basin (Area C/West Block 9), offshore South Africa. Mar Pet Geo

Thomson K (1998) When did the Falklands rotate? Mar Pet Geol 15:723–736

Tissot BP, Welte DH (1978) Petroleum formation and occurrence. Springer, Berlin

Tissot B, Welte DH (1984) Petroleum formation and occurrence, 2nd edn. Springer Verlag, Berlin

Van der Merwe R, Fouché J (1992) Inversion tectonics in the Bredasdorp basin, offshore South Africa. In: de Wit MJ, Ransome IGD (eds) Inversion tectonics of the Cape Fold Belt, Karoo and Cretaceous Basins of Southern Africa. Balkema, Rotterdam, pp 51–59

Viljoen JHA, Stapelberg FDJ, Cloete M (2010) Technical Report on the geological storage of carbon dioxide in South Africa. Pretoria, Council for Geoscience, p 238

Waples DW, Ramly M, and Leslie W (1995) Implications of vitrinite-reflectance suppression for the tectonic and thermal history of the Malay Basin. Bul Geo Soc Mal 37:269–284